Nonmonotonic spin relaxation and decoherence in graphene quantum dots with spin-orbit interactions

Marco O. Hachiya,[1] Guido Burkard,[2] and J. Carlos Egues[1]
[1]*Instituto de Física de São Carlos, Universidade de São Paulo, 13560-970 São Carlos, São Paulo, Brazil*
[2]*Department of Physics, University of Konstanz, D-78457 Konstanz, Germany*
(Received 19 July 2013; revised manuscript received 20 February 2014; published 19 March 2014)

We investigate the spin relaxation and decoherence in a single-electron graphene quantum dot with Rashba and intrinsic spin-orbit interactions. We derive an effective spin-phonon Hamiltonian via the Schrieffer-Wolff transformation in order to calculate the spin relaxation time T_1 and decoherence time T_2 within the framework of the Bloch-Redfield theory. In this model, the emergence of a nonmonotonic dependence of T_1 on the external magnetic field is attributed to the Rashba spin-orbit coupling-induced anticrossing of opposite spin states. A rapid decrease of T_1 occurs when the spin and orbital relaxation rates become comparable in the vicinity of the spin-mixing energy-level anticrossing. By contrast, the intrinsic spin-orbit interaction leads to a monotonic magnetic field dependence of the spin relaxation rate which is caused solely by the direct spin-phonon coupling mechanism. Within our model, we demonstrate that the decoherence time $T_2 \simeq 2T_1$ is dominated by relaxation processes for the electron-phonon coupling mechanisms in graphene up to leading order in the spin-orbit interaction. Moreover, we show that the energy anticrossing also leads to a vanishing pure spin dephasing rate for these states for a super-Ohmic bath.

DOI: 10.1103/PhysRevB.89.115427 PACS number(s): 03.67.Lx, 76.60.Es, 73.22.Pr

I. INTRODUCTION

Carbon-based materials such as graphene and carbon nanotubes are of recognized importance for their potential spintronic and quantum computation applications. Notably, single-layer graphene, a one-carbon-atom-thick layer arranged in a honeycomb crystal lattice, has attracted much interest in the past decade due to its unique electronic properties [1]. The electron spin degree of freedom in graphene quantum dots makes them promising candidates for universal scalable quantum computing [2,3], which would rely on spin relaxation and decoherence times much longer than the gate operation times [4]. Graphene has a relatively weak hyperfine interaction and spin-orbit (SO) couplings. A graphene sheet is composed naturally of 99% of ^{12}C with nuclear spin 0, and of 1% ^{13}C with nuclear spin 1/2, leading to long dephasing times in carbon-based quantum dots due to a weak hyperfine interaction [5,6]. Thus graphene emerges as a good candidate to host a spin qubit, in contrast to GaAs quantum dots, whose spin dynamics is strongly modified by the nuclear spin bath. Moreover, the weak SO couplings in graphene generate a spin splitting on the order of tens of μeV due to the low atomic weight of carbon atoms [7,8]. Long spin relaxation times are expected since the mechanisms that enable relaxation channels arise as a combined effect of nonpiezoelectric electron-phonon interactions and weak SO coupling.

Despite the lack of measurements of the spin relaxation and dephasing times in graphene quantum dots, experimental results have already been reported in a two-electron ^{13}C nanotube double quantum dot [9] that has been isotopically enriched. These results showed a nonmonotonic magnetic field dependence of the spin relaxation time near the energy anticrossing. In this case, the spin relaxation minimum is related to the coupling between the electron spin in the quantum dot and the nanotube deflection [10,11].

In this paper, we derive a spin-phonon Hamiltonian using the Schrieffer-Wolff transformation for all mechanisms of electron-phonon and spin-orbit for a circular graphene quantum dot, Fig. 1. This effective Hamiltonian captures the combined effect of the SO interaction and electron-phonon-induced potential fluctuations. Within the Bloch-Redfield theory, we find that a nonmonotonic behavior of the spin relaxation time occurs as a function of the external magnetic field around the spin-mixing energy-level anticrossing by the Rashba SO coupling in combination with the deformation potential and bond-length change electron-phonon mechanisms. We predict that the minimum of the spin relaxation time T_1 could be experimentally observed in graphene quantum dots. This energy anticrossing takes place between the first two excited energy levels at the accidental degeneracy for a certain value $\mathbf{B}^*$ of the external magnetic field. We treat the accidental degeneracy mixed by the Rashba SO coupling using degenerate-state perturbation theory. T_1 strongly decreases at the energy anticrossing, reaching the same order as the orbital relaxation time [12–14]. In contrast with carbon nanotubes, the intrinsic SO does not couple these states due to the selection rules in a circular quantum dot, exhibiting a monotonic magnetic field dependence of T_1 due to direct

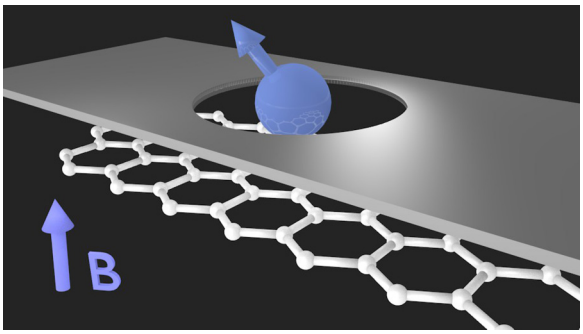

FIG. 1. (Color online) Schematic of a gate-tunable circular graphene quantum dot setup. A homogeneous magnetic field is applied perpendicularly to the gapped graphene sheet. A metallic gate put on top of the graphene defines the confinement potential for a single electron. The figure is not drawn to scale.

spin-phonon coupling (deflection coupling mechanism). Thus we find that different SO coupling mechanisms lead to distinct spin relaxation times as a function of magnetic field. Hence our work also opens up a possibility to probe the spin-orbit couplings in graphene. We also demonstrate that pure spin dephasing rates vanish in the leading order of the electron-phonon interaction and SO interactions causing a decoherence dominated by relaxation processes, i.e., $T_2 = 2T_1$. We find that the influence of the admixture mechanism on the spin decoherence time can compete with the contribution of the nuclear spin bath depending on the value of $\mathbf{B}$. This in contrast with GaAs quantum dots where the hyperfine interaction is the dominant mechanism which strongly reduces the decoherence time in all regimes of $\mathbf{B}$. Moreover, we find a vanishing spin dephasing rate for a super-Ohmic bath as a general property of the energy anticrossing spectrum.

This paper is organized as follows: In Sec. II, we introduce the model to describe a circular graphene quantum dot. In Sec. III, we derive the effective spin-phonon Hamiltonian. In Sec. IV, we present a calculation of the spin relaxation time T_1 within the Bloch-Redfield theory. In Sec. V, we discuss the vanishing spin dephasing rate within our model. Finally, we summarize our results and draw our conclusions in Sec. VI.

II. THE MODEL

In this section, we introduce the model for a circular and gate-tunable graphene quantum dot. (See Fig. 1.) Within our model, we consider a gapped graphene taking into account electron-phonon coupling mechanisms and spin-orbit interactions. We also analyze the energy spectrum of the quantum dot and its energy-level degeneracy. The degenerate levels are mixed by the Rashba SO coupling, and the energy crossings are removed using the standard degenerate perturbation theory.

A. Graphene quantum dots

The low-energy effective Hamiltonian for graphene is analogous to the two-dimensional massless Dirac equation. The characteristic linear dispersion for massless fermions occurs at the two nonequivalent points K and K' (valleys), in the honeycomb lattice Brillouin zone. The graphene energy bands in the vicinity of these high-symmetry points constitute a solid-state realization of relativistic quantum mechanics. However, confining electrons in graphene quantum dots is a difficult task, since the particles tend to escape from the electrostatic confinement potential due to Klein tunneling. This problem can be overcome by putting graphene on top of a substrate, such as SiC [15] and BN [16,17], that induces a nonequivalent potential for each atom of the two carbon sublattices and adds a mass term to the Hamiltonian [18]. The sublattice $A(B)$ will feel a potential parametrized by $+(-)\Delta$ which breaks inversion symmetry, opening a gap 2Δ in the electron-hole energy spectrum. Combined with the mass term, an external magnetic field $\mathbf{B}$ is necessary to break the time-reversal symmetry and lift the valley degeneracy. Thus it is reasonable to confine a single electron in a quantum dot with the restriction of its being localized in a single valley [19,20].

Consider then a circular and gate-tunable graphene quantum dot in an external magnetic field with SO interactions and the electron-phonon interaction described by the following low-energy Hamiltonian for the K valley [18],

$$\mathcal{H} = \mathcal{H}_d + \mathcal{H}_Z + \mathcal{H}_{\text{SO}} + \mathcal{H}_{\text{ph}} + \mathcal{H}_{\text{e-ph}}, \tag{1}$$

with the quantum dot Hamiltonian $\mathcal{H}_d$ and the Zeeman term $\mathcal{H}_Z$, respectively, given by

$$\mathcal{H}_d = \hbar v_F \boldsymbol{\Pi}\cdot\boldsymbol{\sigma} + U(r) + \Delta\sigma_z, \quad \mathcal{H}_Z = \tfrac{1}{2} g\mu_B \mathbf{B}\cdot\mathbf{s}, \tag{2}$$

where $\boldsymbol{\Pi} = \mathbf{p} - e\mathbf{A}$ is the canonical momentum. The vector potential is chosen such that $\mathbf{B} = \nabla\times\mathbf{A} = (0,0,B)$, i.e., perpendicular to the graphene sheet. Here, $v_F = 10^6$ m/s is the Fermi velocity, $U(r) = U_0\Theta(r-R)$ is the circular-shaped electrostatic potential, with $\Theta(x) = 1$ for $x \geqslant 0$ and $\Theta(x) = 0$ for $x < 0$. The operator $\boldsymbol{\sigma}$ acts on the pseudospin subspace (A, B sublattices), while $\mathbf{s}$ acts on the real spin. Both operators $\boldsymbol{\sigma}$ and $\mathbf{s}$ are represented by Pauli matrices.

The SO Hamiltonian for the K valley reads [21]

$$\mathcal{H}_{\text{SO}} = \mathcal{H}_i + \mathcal{H}_R = \lambda_i\sigma_z s_z + \lambda_R(\sigma_x s_y - \sigma_y s_x), \tag{3}$$

where $\mathcal{H}_i$ and $\mathcal{H}_R$ denote the intrinsic and Rashba SO effective Hamiltonians [7], respectively. The intrinsic SO coupling originates from the local atomic SO interaction. At first, only the contribution from the σ-π orbital coupling was considered, resulting in a second-order term to the intrinsic SO coupling strength λ_{i} [8]. However, some d orbitals hybridize with p_z forming a π band that gives a first-order contribution which plays a major role in the spin-orbit-induced gap [22]. The Rashba SO coupling, also called the extrinsic contribution, arises when an electric field is applied perpendicular to the graphene sheet. The major contribution of the SO coupling λ_R comes from the σ-π hybridization [8], in contrast with the intrinsic case. The Rashba SO could also be enhanced by curvature effects in the graphene sheet [23].

The free phonon Hamiltonian is given by

$$\mathcal{H}_{\text{ph}} = \sum_{\mathbf{q},\mu} \hbar\omega_{\mathbf{q},\mu} b^\dagger_{\mathbf{q},\mu} b_{\mathbf{q},\mu}, \tag{4}$$

with the dispersion relation $\omega_{\mathbf{q},\mu} = s_\mu|\mathbf{q}|^m$, where s_μ is the sound velocity. Here, μ denotes the phonon mode and $m = 1,2$ depending on the type of phonon branch.

Finally, we have the electron-phonon interaction $\mathcal{H}_{\text{e-ph}}$. We consider long-wavelength acoustic phonons represented by two main mechanisms: the deformation potential and the bond-length change mechanism [24]. The former is an effective potential generated by static distortions of the lattice. It is represented in the sublattice space as a diagonal energy shift in the band structure. The latter are off-diagonal terms due to modifications of the bond length between neighboring carbon atoms, which cause changes in the hopping amplitude. The electron-phonon interaction in the sublattice space is given by [24]

$$\mathcal{H}_{\text{e-ph}} = \sum_{q,\mu} \frac{q}{\sqrt{A\rho\omega_{q,\mu}}} \begin{pmatrix} g_1 a_1 & g_2 a_2^* \\ g_2 a_2 & g_1 a_1 \end{pmatrix} (e^{i\mathbf{qr}} b^\dagger_{q,\mu} - e^{-i\mathbf{qr}} b_{q,\mu}), \tag{5}$$

where g_1 and g_2 are the deformation potential and bond-length change coupling constants. Here, A is the area of the graphene layer and ρ is the mass area density. The constants a_1,a_2

TABLE I. Electron-phonon constants and sound velocities for longitudinal (LA) and transverse (TA) acoustic phonons. The phonon emission angle is denoted by ϕ_q.

	a_1	a_2	s_μ (10^4 m/s)
LA	i	$ie^{2i\phi_q}$	1.95[a]
TA	0	$e^{2i\phi_q}$	1.22[a]

[a]From Ref. [25].

and the sound velocities $s_{\rm LA}, s_{\rm TA}$ for the longitudinal-acoustic ($\mu = {\rm LA}$) and transverse-acoustic ($\mu = {\rm TA}$) modes are given in Table I. Both phonon branches have a linear dispersion relation given by $\omega_{\mathbf{q},\mu} = s_\mu |\mathbf{q}|$. Optical phonons are not taken into account in this work, since their energies do not match the Zeeman splitting for typical laboratory fields. Also, we do not consider out-of-plane phonons ($\mu = {\rm ZA}$) since they contribute via a second-order process. Nevertheless, this type of phonon will be discussed further below in connection with the deflection coupling mechanism. Notice that the electron-phonon interaction is spin independent and can only cause a spin relaxation when assisted by the SO interaction.

In the following, we analyze the bare quantum dot spectrum and perform a perturbation theory calculation for degenerate levels treating the SO Hamiltonian as a perturbative term.

B. Degenerate-state perturbation theory

In order to calculate T_1 and T_2, we use the quantum dot eigenstates perturbed by the SO interaction. Before doing so, we have to get rid of the degeneracies in the quantum dot spectrum by applying degenerate-state perturbation theory. This procedure makes it clearer to define which states constitute our spin qubit and where the spin relaxation occurs.

Due to the selection rules for the matrix elements of the SO interaction [26], only the Rashba SO term couples states from the degenerate subspace. Thus we intend to find a linear combination of eigenstates from the degenerate subspace of the quantum dot such that these states are not coupled by the Rashba SO Hamiltonian $\mathcal{H}_R$.

Consider then, first the bare quantum dot Hamiltonian in the K valley $\mathcal{H}_d$, with $\mathcal{H}_d|j,\nu,s\rangle = E_{j,\nu}|j,\nu,s\rangle$ and the quantum dot wave functions [18]

$$\langle r,\phi|j,\nu,s\rangle = \psi_{j,\nu,s}(r,\phi) = e^{i(j-1/2)\phi}\begin{pmatrix} \chi_A^{j,\nu,s}(r) \\ \chi_B^{j,\nu,s}(r)e^{i\phi}\end{pmatrix}. \quad (6)$$

The spinor components $\chi_{A,B}^{j,\nu,s}(r)$ are proportional to the confluent hypergeometric functions and are described by the set $j,\nu,$s, where we introduce the angular ($j = \pm 1/2, \pm 3/2, \ldots$), radial ($\nu = 1,2,3,\ldots$), and spin $s = \uparrow,\downarrow$ quantum numbers.

Matching the spinors at $r = R$ results in a transcendental equation for the eigenvalues $E_{\rm j,\nu}$ which can be obtained numerically [18]. Since we are going to calculate the spin relaxation rates due to transitions between the lowest three energy levels of the quantum dot, we restrict ourselves to the analysis of the subspace $\{|1/2,1,\downarrow\rangle, |1/2,1,\uparrow\rangle, |-1/2,1,\downarrow\rangle\}$. Including the Zeeman spin splitting, it leads to a crossing of the energy levels $E_{1/2,1,\uparrow}$ and $E_{-1/2,1,\downarrow}$ for a certain magnetic field $\mathbf{B}^*$ depending on the size of the quantum dot. The ground state $|1/2,1,\downarrow\rangle$ is not degenerate for any value of $\mathbf{B}$. The Rashba SO interaction $\mathcal{H}_R$ couples two of these states $|1/2,1,\uparrow\rangle$ and $|-1/2,1,\downarrow\rangle$ due to its selection rule for the angular quantum number j [26], which is given by $|j - j'| = 1$. By contrast, the intrinsic SO interaction $\mathcal{H}_{\rm i}$ does not couple them since its selection rule is $|j - j'| = 0$. Now, we have to find an appropriate linear combination of the states from the degenerate subspace $|1/2,1,\uparrow\rangle, |-1/2,1,\downarrow\rangle$ in which $\mathcal{H}_R$ becomes diagonal in order to remove the accidental energy-level degeneracy from the denominator in the usual nondegenerate perturbation theory. Then, performing standard degenerate-state perturbation theory, we obtain the zero-order eigenstates for the three lowest-energy levels given by

$$\begin{bmatrix}|\gamma_0\rangle \\ |\gamma_1\rangle \\ |\gamma_2\rangle\end{bmatrix} = \begin{bmatrix}1 & 0 & 0 \\ 0 & \cos(\vartheta/2)e^{i\delta} & -\sin(\vartheta/2) \\ 0 & \sin(\vartheta/2)e^{i\delta} & \cos(\vartheta/2)\end{bmatrix}\begin{bmatrix}|1/2,1,\downarrow\rangle \\ |1/2,1,\uparrow\rangle \\ |-1/2,1,\downarrow\rangle\end{bmatrix}, \quad (7)$$

with the associated first-order eigenvalues

$$E_{\gamma_0} = E_{1/2,1} - \frac{\hbar\omega_Z}{2}, \quad E_{\gamma_1,\gamma_2} = \epsilon_+ \mp \sqrt{\epsilon_-^2 + |\Delta_{\rm SO}|^2}, \quad (8)$$

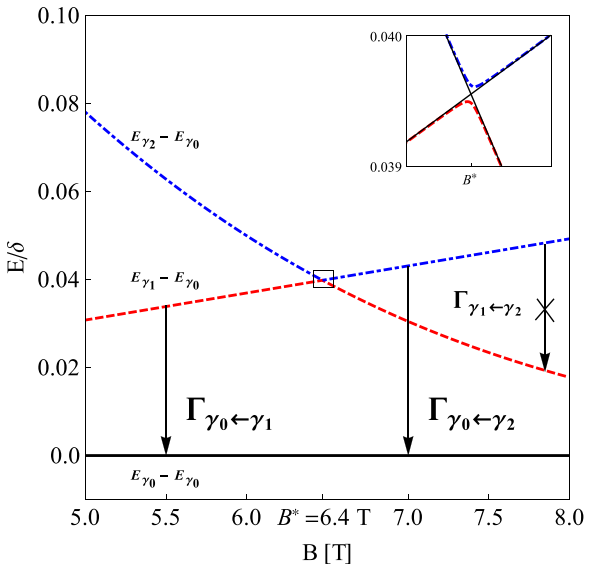

FIG. 2. (Color online) Magnetic field dependence of the energy difference between the perturbed three lowest-energy levels and the ground state in a circular graphene quantum dot. Our spin qubit is composed by the ground state and the first excited state with opposite spin orientations. Sequentially from bottom to top, $E_{\gamma_0} - E_{\gamma_0}$ (solid), $E_{\gamma_1} - E_{\gamma_0}$ (dashed), and $E_{\gamma_2} - E_{\gamma_0}$ (dotted-dashed). The Rashba SO interaction-induced anticrossing of the bare quantum dot states $E_{1/2,1,\uparrow}$ and $E_{-1/2,1,\downarrow}$, at $B = B^*$ (solid lines in the inset). The spin relaxation rate takes place between the states $|\gamma_0\rangle$ and $|\gamma_1\rangle$ ($\Gamma_{\downarrow\uparrow} = \Gamma_{\gamma_0\leftarrow\gamma_1}$) before the anticrossing, and between the states $|\gamma_0\rangle$ and $|\gamma_2\rangle$ ($\Gamma_{\downarrow\uparrow} = \Gamma_{\gamma_0\leftarrow\gamma_2}$) after the anticrossing. Notice that there can be also spin relaxation from $|\gamma_2\rangle$ to $|\gamma_1\rangle$ followed by a orbital relaxation from $|\gamma_1\rangle$ to $|\gamma_0\rangle$ after the anticrossing. Nevertheless, we neglect this contribution since we can show that $\Gamma_{\gamma_1\leftarrow\gamma_2} \ll \Gamma_{\gamma_0\leftarrow\gamma_2}$ (higher-order process). Inset: Blowup of the energy levels in the vicinity of the crossing region.

plotted in Fig. 2. We define $\epsilon_+ = (E_{1/2,1} + E_{-1/2,1})/2$ and $\epsilon_- = (E_{1/2,1} - E_{-1/2,1} + \hbar\omega_Z)/2$, and $\hbar\omega_Z = g\mu_B B$ is the Zeeman energy splitting. Here, $\Delta_{\rm SO} = \langle 1/2,1,\uparrow|\mathcal{H}_R|-1/2,1,\downarrow\rangle = 4\pi i\lambda_R \int dr\, r\, \chi_A^{1/2,1}(r)\chi_B^{-1/2,1}(r)$, $\tan\vartheta = \Delta_{\rm SO}/\epsilon_-$, and $\tan\delta = {\rm Im}[\Delta_{\rm SO}]/{\rm Re}[\Delta_{\rm SO}]$, where ${\rm Im}[x]$ is the imaginary part and ${\rm Re}[x]$ the real part of x. As a result, the Rashba SO induces an energy gap $2\Delta_{\rm SO}$ at the energy anticrossing ($\epsilon_- = 0$), as shown in Fig. 2. We have two dominant spin components for $|\gamma_1\rangle$ and $|\gamma_2\rangle$ depending on whether the spin relaxation takes place before or after the energy anticrossing region. Before the energy anticrossing, $\Delta_{\rm SO}/\epsilon_- > 0$, $|\gamma_1\rangle \approx |1/2,1,\uparrow\rangle + O(\Delta_{\rm SO}/\epsilon_-)$, and $|\gamma_2\rangle \approx |-1/2,1,\downarrow\rangle + O(\Delta_{\rm SO}/\epsilon_-)$. Increasing the magnetic field we go through the energy anticrossing region such that $\vartheta \to \pi/2$ when $\epsilon_- = 0$. As a result, the states from the degenerate subspace hybridize $|\gamma_1\rangle \approx (|1/2,1,\uparrow\rangle - |-1/2,1,\downarrow\rangle)/\sqrt{2}$ and $|\gamma_2\rangle \approx (|1/2,1,\uparrow\rangle + |-1/2,1,\downarrow\rangle)/\sqrt{2}$. After the energy anticrossing, $\Delta_{\rm SO}/\epsilon_- < 0$, $|\gamma_1\rangle \approx |-1/2,1,\downarrow\rangle + O(\Delta_{\rm SO}/\epsilon_-)$, and $|\gamma_2\rangle \approx |1/2,1,\uparrow\rangle + O(\Delta_{\rm SO}/\epsilon_-)$. Thus before the energy anticrossing, the spin relaxation takes place between $|\gamma_1\rangle \to |\gamma_0\rangle$ and after the energy anticrossing between $|\gamma_2\rangle \to |\gamma_0\rangle$. At the energy anticrossing, the spin up and spin down are equivalently mixed and the orbital relaxation rate becomes comparable to the spin relaxation rate, since the latter is a higher-order process assisted by the SO interaction [12–14]. These results will be used to study the energy relaxation with spin flip between excited states and the ground state.

III. EFFECTIVE SPIN-PHONON HAMILTONIAN

The electron-phonon coupling allows for energy relaxation between the Zeeman levels via the admixed states with opposite spin due to the presence of the SO interaction. To study this admixture mechanism we derive an effective Hamiltonian describing the coupling of spin to potential fluctuations generated by the electron-phonon coupling. We perform a Schrieffer-Wolff transformation in order to eliminate the SO interaction in leading order [27,28],

$$\widetilde{\mathcal{H}} = e^{\mathcal{S}}\mathcal{H}e^{-\mathcal{S}} = \mathcal{H}_d + \mathcal{H}_Z + \mathcal{H}_{\rm ph} + \mathcal{H}_{\text{e-ph}} + [\mathcal{S},\mathcal{H}_{\text{e-ph}}], \quad (9)$$

where we have retained terms up to $O(\mathcal{H}_{\rm SO})$ [29]. The operator $\mathcal{S}$ obeys the commutator $[\mathcal{H}_d + \mathcal{H}_Z,\mathcal{S}] = \mathcal{H}_{\rm SO}$, with $\mathcal{S} \sim O(\mathcal{H}_{\rm SO})$. The term $[\mathcal{S},\mathcal{H}_{\text{e-ph}}]$ represents the coupling of the electron spin to the charge fluctuations induced by the electron-phonon interaction via the SO interaction (admixture mechanism). The operator $\mathcal{S}$ can be rewritten as $\mathcal{S} = (L_d + L_Z)^{-1}\mathcal{H}_{\rm SO}$, where $\hat{L}_i$ is the Liouvillian superoperator defined as $L_i A = [\mathcal{H}_i, A]$, where A denotes an arbitrary operator. Here, we make the distinction $\mathcal{S} = \mathcal{S}^R + \mathcal{S}^i$, where $\mathcal{S}^i \propto \lambda_i$ and $\mathcal{S}^R \propto \lambda_R$.

For the Rashba SO coupling, we have to consider the basis $\{|\gamma_1\rangle,|\gamma_2\rangle\}$ calculated in Sec. II B using perturbation theory for the degenerate levels. As explained in Sec. II B, we are interested in transitions from the excited states $|\gamma_k\rangle$ to the ground state $|\gamma_0\rangle$. In this case, we calculate the matrix element of the effective spin-phonon Hamiltonian $\langle\gamma_0|\mathcal{H}^R_{\text{s-ph}}|\gamma_k\rangle = \langle\gamma_0|\mathcal{H}_{\text{e-ph}} + [\mathcal{S}^R,\mathcal{H}_{\text{e-ph}}]|\gamma_k\rangle$, where $\gamma_k = \gamma_1,\gamma_2$. We find that

$$\begin{aligned}\langle\gamma_0|\mathcal{H}^R_{\text{s-ph}}|\gamma_k\rangle = {}& \langle\gamma_0|\mathcal{H}_{\text{e-ph}}|\gamma_k\rangle \\ &+ \sum_{n,s\neq\gamma_0} \frac{\Omega_1(\gamma_0,n,\gamma_k)}{E_{\gamma_0} - E_n} \\ &+ \sum_{n,s\neq\mathfrak{D}} \frac{\Omega_2(\gamma_0,n,\gamma_k)}{E_{\gamma_k} - E_n}, \end{aligned} \quad (10)$$

where $n = (j,\upsilon)$ and the degenerate subspace is given by $\mathfrak{D} = \{|1/2,1,\uparrow\rangle,|-1/2,1,\downarrow\rangle\}$. Here, we have defined the product of the matrix elements as

$$\Omega_1(\gamma_0;n,s;\gamma_k) = \langle\gamma_0|\mathcal{H}_R|n,s\rangle\langle n,s|\mathcal{H}_{\text{e-ph}}|\gamma_k\rangle, \quad (11)$$

$$\Omega_2(\gamma_0;n,s;\gamma_k) = \langle\gamma_0|\mathcal{H}_{\text{e-ph}}|n,s\rangle\langle n,s|\mathcal{H}_R|\gamma_k\rangle. \quad (12)$$

The matrix elements of the Rashba SO coupling give the selection rule $|j - j'| = 1$ [30]. These transitions are compatible with the selection rules of the electron-phonon interaction mechanisms depending on the order of the dipole expansion considered in the term $e^{\pm i\mathbf{q}\cdot\mathbf{r}}$ [26]. In this instance, the selection rules match $|j - j'| = 1$ for the first order and zero order of the dipole expansion of the deformation potential (LA) and bond-length change (LA, TA), respectively.

For the intrinsic SO, the matrix element of the spin-phonon Hamiltonian is given by $\langle n_0,\downarrow|\mathcal{H}^i_{\text{s-ph}}|n_0,\uparrow\rangle = \langle n_0,\downarrow|[\mathcal{S}^i,\mathcal{H}_{\text{e-ph}}]|n_0,\uparrow\rangle$, with the ground state set of angular and radial quantum numbers $n_0 = (1/2,1)$, since $\mathcal{H}_i$ does not connect the quantum states related with the crossed energy levels. This matrix element is trivially zero since $\mathcal{H}_i \propto s_z$. Here we demonstrate that this contribution vanishes for any orientation of $\mathbf{B}$. Explicitly, we have

$$\langle n_0|\mathcal{H}^i_{\text{s-ph}}|n_0\rangle \propto \sum_{n'\neq n_0} \delta_{j,j'}\left(N^{AA}_{n_0n'} - N^{BB}_{n_0n'}\right), \quad (13)$$

where $N^{AA}_{nn'} = \int dr\, r\, \chi^n_A(r)\chi^{n'}_A(r)$ and $N^{BB}_{nn'} = \int dr\, r\, \chi^n_B(r)\chi^{n'}_B(r)$. The selection rule of the intrinsic SO is $|j - j'| = 0$, which is compatible with the zero order and first order of the dipole expansion of the deformation potential (LA) and bond-length change (LA, TA), respectively. The functions $\chi^n_A(r)$ and $\chi^n_B(r)$ are, respectively, purely real and purely imaginary. Thus $\mathcal{H}^i_{\text{s-ph}}$ can be rewritten as proportional to $\langle j,\upsilon|j,\upsilon'\rangle$ with $\upsilon \neq \upsilon'$, which is identically zero. Consequently, the admixture mechanism due to the intrinsic SO does not contribute to the spin relaxation and dephasing process within our model.

In addition to the admixture mechanism, the spin relaxation can also take place due to the direct coupling of spin and local out-of-plane deformations of the graphene sheet (deflection coupling mechanism) [11,26]. Assuming small amplitudes for the displacement compared to the phonon wavelength, the normal vector to the graphene sheet is $\hat{n}(z) \approx \hat{z} + \nabla u(x,y)$. The displacement operator is given by $u_z = \sqrt{1/A\rho\omega_q}(e^{i\mathbf{qr}}b^\dagger - e^{-i\mathbf{qr}}b)$, where we consider linear and quadratic behaviors to the dispersion relation $\hbar\omega_q = \hbar sq + \hbar\eta q^2$, where $\eta = \sqrt{\kappa/\rho}$, with the bending rigidity $\kappa = 1.1$ eV. The matrix element of the effective Hamiltonian containing only the terms connecting

the Zeeman levels of the ground state reads

$$\langle n_0,\downarrow|\mathcal{H}^{\mathrm{ZA}}_{\text{s-ph}}|n_0,\uparrow\rangle = \frac{i\lambda_{\mathrm{i}}}{\sqrt{A\rho\omega_q}}(q_x+iq_y)\big(N^{AA}_{n_0n_0}+N^{BB}_{n_0n_0}\big), \tag{14}$$

where $s_{\mathrm{ZA}} = 0.25\times10^3$ m/s is the sound velocity. Here, only the lowest order of the dipole approximation gives a nonzero contribution. The spin-phonon terms presented here will be used to calculate the spin relaxation and dephasing rates in the following sections.

IV. SPIN RELAXATION RATES

In this section, we calculate the spin relaxation time using the effective spin-phonon Hamiltonian derived in the previous section. First, we introduce the Bloch-Redfield theory [31,32], which allows us to derive the general expression for the spin relaxation and decoherence times.

Consider a general Hamiltonian given by $\mathcal{H} = \mathcal{H}_S + \mathcal{H}_B + \mathcal{H}_{SB}$, where $\mathcal{H}_S$ describes the system, $\mathcal{H}_B$ a reservoir in thermal equilibrium (bath), and $\mathcal{H}_{SB}$ describes the interaction between them. This general Hamiltonian $\mathcal{H}$ is analogous to the one derived in Sec. III for all electron-phonon mechanisms and SO interactions via the mapping $\mathcal{H}_S \to \mathcal{H}_d + \mathcal{H}_Z$, $\mathcal{H}_B \to \mathcal{H}_{\text{ph}}$ and $\mathcal{H}_{SB} \to \mathcal{H}_{\text{s-ph}}$. The system and the bath are uncorrelated initially, i.e., their density matrices ρ can be separated as $\rho(0) = \rho_S(0)\rho_B(0)$. Nevertheless, as time goes by, the system and the bath become correlated via the interaction term $\mathcal{H}_{\text{s-ph}}$. This system dynamics is described by an equation of motion for the density matrix in the interaction picture ($\hat{\rho} = e^{i(\mathcal{H}_d+\mathcal{H}_Z+\mathcal{H}_{\text{ph}})t/\hbar}\rho e^{-i(\mathcal{H}_d+\mathcal{H}_Z+\mathcal{H}_{\text{ph}})t/\hbar}$) with the bath variables traced out $\hat{\rho}_S = \mathrm{Tr}_B[\hat{\rho}]$ as

$$\frac{d}{dt}\hat{\rho}_S(t) = -\frac{i}{\hbar}\int_0^t dt'\mathrm{Tr}_B[\hat{\mathcal{H}}_{\text{s-ph}}(t),[\hat{\mathcal{H}}_{\text{s-ph}}(t'),\hat{\rho}_S(t')\hat{\rho}_B(0)]]. \tag{15}$$

This equation of motion for the reduced density matrix is called the Nakajima-Zwanzig equation [32]. If we assume that the coupling system bath is weak, this equation can be further simplified by neglecting terms up to $O(\mathcal{H}^2_{\text{s-ph}})$ in Eq. (15), which is equivalent to approximating the density matrix in the integral as $\rho(t) = \rho_S(t)\rho_B(0) + O(\mathcal{H}_{\text{s-ph}})$ (Born approximation). Considering a phonon bath, we assume that the time evolution of the $\rho_S(t)$ depends only on its present value and not on its past state (Markov approximation), i.e., $\hat{\rho}(t') \to \hat{\rho}(t)$ in the integral of Eq. (15). Taking the matrix elements of Eq. (15) between the eigenstates of $\mathcal{H}_S$, we have that

$$\frac{d}{dt}\hat{\rho}_{Smn}(t) = -\frac{i}{\hbar}\omega_{mn}\rho_{Smn} - \sum_{k,l}R_{nmkl}\rho_{Skl}(t), \tag{16}$$

where $\rho_{Smn} = \langle m|\rho_S|n\rangle$ and $\omega_{nm} = \omega_n - \omega_m$. The term R_{nmkl} is the Redfield tensor

$$R_{nmkl} = \delta_{nm}\sum_r\Gamma^+_{nrrk} + \delta_{nk}\sum_r\Gamma^-_{lrrm} - \Gamma^+_{lmnk} - \Gamma^-_{lmnk}, \tag{17}$$

where $\Gamma^+_{lmnk} = \int_0^\infty dt e^{-i\omega_{nk}t}\overline{\langle l|\mathcal{H}_{\text{s-ph}}|m\rangle\langle n|\mathcal{H}_{\text{s-ph}}(t)|k\rangle}$, with $\Gamma^+_{lmnk} = (\Gamma^-_{knml})^*$ and $\mathcal{H}_{\text{s-ph}}(t) = \exp(i\mathcal{H}_Bt/\hbar)\mathcal{H}_{\text{s-ph}}\exp(-i\mathcal{H}_Bt/\hbar)$. Here, the overbar denotes the average over a phonon bath in thermal equilibrium at temperature T. Using Eq. (16) in the secular approximation where R_{nmkl} is approximately given by a diagonal tensor and $\langle dS_i/dt\rangle = \mathrm{Tr}[(d\rho/dt)S_i]$ with $i = x,y,z$, we can derive the differential equation describing time evolution of the average values of the spin components, also known as Bloch equations. The solution for the $\langle S_z\rangle$ component with a magnetic field applied along the same direction is $\langle S_z\rangle(t) = S^0_z - [S^0_z - S_z(0)]e^{-t/T_1}$, where S^0_z is the equilibrium spin polarization (ensemble of spin-down electrons)and $S_z(0)$ is the initial nonequilibrium spin alignment considered in the problem (ensemble of spin-up electrons).

Explicitly, the spin relaxation rate is given by [32]

$$\Gamma_{\downarrow\uparrow} = \frac{1}{T_1} = 2\,\mathrm{Re}\big(\Gamma^+_{\gamma_0\gamma_k\gamma_k\gamma_0} + \Gamma^+_{\gamma_k\gamma_0\gamma_0\gamma_k}\big). \tag{18}$$

Equation (18) can be simplified to

$$\frac{1}{T_1} = \frac{2\pi}{\hbar}\sum_q|\langle\gamma_0|\mathcal{H}_{\text{s-ph}}|\gamma_k\rangle|^2\delta\big(\hbar\omega_{\gamma_0\gamma_k} - \hbar\omega_q\big)\coth\left(\frac{\hbar\omega_{\gamma_0\gamma_k}}{2k_bT}\right). \tag{19}$$

The spin relaxation rate is then calculated combining Eqs. (19) and (10). The contribution due to the deformation potential (LA) combined with the Rashba SO coupling is given by

$$\Gamma^{g_1:\mathrm{LA}}_{\gamma_0\leftarrow\gamma_k} = \frac{\pi}{2}\frac{g_1^2}{\hbar\rho s^2_{\mathrm{LA}}}\left(\frac{E_{\gamma_k}-E_{\gamma_0}}{\hbar s_{\mathrm{LA}}}\right)^4\int_0^{2\pi}d\phi_q\big[\Lambda^k_i\big(A_{g_1}\big)\big]^2, \tag{20}$$

and those due to the bond-length change mechanism for $\mu =$ LA,TA,

$$\Gamma^{g_2:\mathrm{LA,TA}}_{\gamma_0\leftarrow\gamma_k} = 2\pi\frac{g_2^2}{\hbar\rho s^2_{\mu}}\left(\frac{E_{\gamma_k}-E_{\gamma_0}}{\hbar s_{\mu}}\right)^2\int_0^{2\pi}d\phi_q\big[\Lambda^k_i\big(A_{g_2}\big)\big]^2, \tag{21}$$

where we imply summation over the repeated index $i = 1,2,3$. In the above we have define

$$\Lambda^k_1\big(A_{g_1,g_2}\big) = \lambda^n_1\langle 1/2,1,\downarrow|A_{g_1,g_2}|-1/2,1,\uparrow\rangle\rho_k, \tag{22}$$

$$\Lambda^k_2\big(A_{g_1,g_2}\big) = \sum_{n\neq(1/2,1)}\lambda^n_2\langle 1/2,1,\downarrow|A_{g_1,g_2}|n,\downarrow\rangle \times\langle n,\downarrow|H_R|1/2,1,\uparrow\rangle\sigma_k, \tag{23}$$

$$\Lambda^k_3\big(A_{g_1,g_2}\big) = \sum_{n\neq(1/2,1)}\lambda^n_3\langle 1/2,1,\downarrow|H_R|n,\uparrow\rangle \times\langle n,\uparrow|A_{g_1,g_2}|1/2,1,\uparrow\rangle\sigma_k, \tag{24}$$

where $A_{g_1} = a_1\mathbb{1}_{2x2}$, $A_{g_2} = g_2(\sigma_+a^*_2 + \sigma_-a_2)$, with $\sigma_\pm = (\sigma_x \pm i\sigma_y)/2$. Their respective matrix elements are given by

$$\langle n|A_{g_1}|n'\rangle = M_{nn'}(\delta_{j,j'+1}e^{-i\phi_q} + \delta_{j,j'-1}e^{+i\phi_q}), \tag{25}$$

with $M_{nn'} = \int dr\, r^2(\chi^{n*}_A\chi^{n'}_A + \chi^{n*}_B\chi^{n'}_B)$, and

$$\langle n|A_{g_2}|n'\rangle = \big(g_2a^*_2\delta_{j,j'+1}N^{AB}_{nn'} + g_2a_2\delta_{j,j'-1}N^{AB}_{n'n}\big), \tag{26}$$

where $N^{AB}_{nn'} = \int dr\, r\chi^n_A(r)\chi^{n'}_B(r)$. Here, $\rho_{\gamma_1} = -\sin(\vartheta/2)$, $\sigma_{\gamma_1} = \cos(\vartheta/2)$ and $\rho_{\gamma_2} = \cos(\vartheta/2)$, $\sigma_{\gamma_2} = \sin(\vartheta/2)$. The

energy-dependent denominators are given by $\lambda_1^n = 1$, $\lambda_2^n = 1/E_k - E_n + g\mu_B B/2$, and $\lambda_3^n = 1/E_{1/2,1} - E_n - g\mu_B B/2$.

As stated in Sec. II B, the energy relaxation accompanied by a spin-flip transition occurs between the states $|\gamma_0\rangle$ and $|\gamma_1\rangle$ before the energy anticrossing $\Gamma_{\downarrow\uparrow} = \Gamma_{\gamma_0\leftarrow\gamma_1}$, and between the states $|\gamma_0\rangle$ and $|\gamma_2\rangle$ after the energy anticrossing $\Gamma_{\downarrow\uparrow} = \Gamma_{\gamma_0\leftarrow\gamma_2}$, for all electron-phonon mechanisms $\Gamma^R_{\downarrow\uparrow} = \Gamma^{g_1:\mathrm{LA}}_{\gamma_0\leftarrow\gamma_k} + \Gamma^{g_2:\mathrm{LA}}_{\gamma_0\leftarrow\gamma_k} + \Gamma^{g_2:\mathrm{TA}}_{\gamma_0\leftarrow\gamma_k}$. Notice that spin relaxation from $|\gamma_2\rangle$ to $|\gamma_0\rangle$ after the anticrossing can be viewed as a two-channel process since there can be spin relaxation from $|\gamma_2\rangle$ to $|\gamma_1\rangle$ followed by a orbital relaxation from $|\gamma_1\rangle$ to $|\gamma_0\rangle$. Nevertheless, we find that $\Gamma_{\gamma_1\leftarrow\gamma_2} \propto O(\mathcal{H}^4_{\mathrm{SO}})$ is a higher-order process in the spin-orbit interaction (see the Appendix). Thus it can be neglected when compared to the direct spin relaxation rate to the ground state $\Gamma_{\gamma_0\leftarrow\gamma_2}$ since $\Gamma_{\gamma_1\leftarrow\gamma_2} \ll \Gamma_{\gamma_0\leftarrow\gamma_2}$.

The contribution from the out-of-plane bending-mode phonons via the deflection coupling mechanism, calculated using Eq. (19) combined with Eq. (14), is

$$\Gamma^{\mathrm{ZA}}_{\downarrow\uparrow} = \frac{4\pi^2}{\rho}\frac{\lambda_i^2}{g\mu_B B}\frac{1}{Q(B)}\left(\frac{-s_{\mathrm{ZA}} + Q(B)}{2\eta}\right)^3 \times \left|\int dr\, r\left(\left|\chi_A^n\right|^2 - \left|\chi_B^n\right|^2\right)\right|^2, \tag{27}$$

where we define $Q(B) = \sqrt{s_{\mathrm{ZA}}^2 + 4\eta(g\mu_B B/\hbar)}$, with $s_{\mathrm{ZA}} = 0.25 \times 10^3$ m/s. In the low magnetic field limit, the term $\Gamma^{\mathrm{ZA}}_{\downarrow\uparrow}$ simplifies to

$$\Gamma^{\mathrm{ZA}}_{\downarrow\uparrow} = \frac{4\pi^2\lambda_i^2}{\rho}\frac{1}{s_{\mathrm{ZA}}^5}(g\mu_B B)^2\left|\int dr\, r\left(\left|\chi_A^n\right|^2 - \left|\chi_B^n\right|^2\right)\right|^2. \tag{28}$$

The magnetic field dependence of $T_1 = (\Gamma^R_{\downarrow\uparrow} + \Gamma^{\mathrm{ZA}}_{\downarrow\uparrow})^{-1}$ with all the mechanisms considered in this work is evaluated numerically and is presented in Fig. 3. It can be observed that at the energy anticrossing region, the spin relaxation time rapidly decreases, characterizing its nonmonotonic behavior induced by an external electric field via the Rashba SO interaction. Notice that if no external electric field is applied, the spin relaxation time is monotonic with contributions from only the intrinsic SO interaction via the deflection coupling mechanism.

Similarly to graphene quantum dots, the spin relaxation rate $\Gamma_{\downarrow\uparrow}$ in carbon nanotube quantum dots also shows a nonmonotonic dependence on the external magnetic field [10,11]. An enhancement of $\Gamma_{\downarrow\uparrow}$ arises due to a singularity in the density of states of the bending-mode phonons with the spin-flip mechanism provided by the SO induced by the nanotube curvature. On the other hand, several dips in $\Gamma_{\downarrow\uparrow}$ are caused by interference of the phonon wave in the cavity formed by the nanotube and the confining potential and due to the interplay between different spin-flip processes [10]. A coupling between the bending-mode phonons and the SO coupling [11] has also been predicted which is similar to the direct spin-phonon coupling derived by us in graphene. In Ref. [11], they show a minimum of T_1 near the SO-induced energy anticrossing that can be associated with the same behavior observed experimentally by Churchill *et al.* [9]. This is a distinct feature compared with graphene quantum dots since the direct spin-phonon coupling does not couple the anticrossing states leading to a monotonic behavior of T_1 as a function of **B**. Nevertheless, we still obtain a T_1 minimum but caused solely by the admixture mechanism.

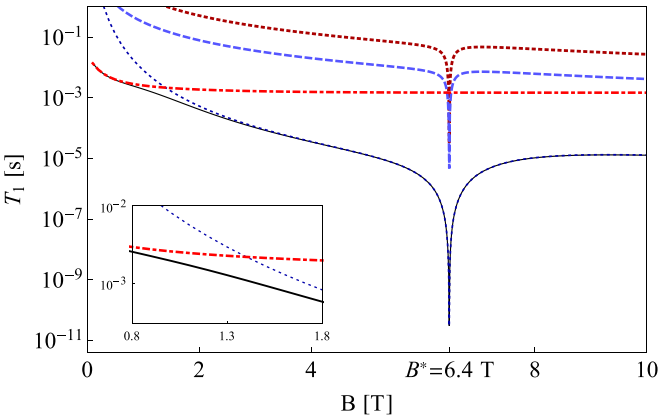

FIG. 3. (Color online) Magnetic field dependence of the spin relaxation time. Parameters used in the numerical evaluation are given in Table II. Contributions from the deformation potential g_1 : LA (dark, dotted), bond-length change mechanism g_2 : LA (dark, dotted) and g_2 : TA (light, dashed), and the out-of-plane phonons ZA (light, dotted-dashed). Dark solid: The sum of all processes. The minimum in T_1 occurs at the energy-level anticrossing at B^*. Inset: Blowup of the low magnetic field regime. Competition between the two electron-phonon dominant mechanisms, deformation potential and bending-mode phonons. The absence of Van Vleck cancellation [26,33–35] leads to a finite value for T_1 in the limit $B \to 0$.

The magnetic field dependence of the spin relaxation rate for each electron-phonon coupling mechanism can be understood using the spectral density of the system-bath

TABLE II. Parameters for the numerical evaluation of the spin relaxation rates. The electron-phonon coupling constants for the deformation potential g_1 and for the bond-length change mechanism g_2 and the coupling strengths for Rashba λ_R for an external electric field E and the intrinsic λ_i SO couplings. The graphene layer is characterized by its mass area density ρ. The quantum dot parameters are its radius R, potential height U_0, and the substrate-induced energy gap Δ. The system is assumed to be in thermal equilibrium with the bath at temperature T.

g_1	30 eV[a]
g_2	1.5 eV[a]
λ_R	11 μeV[b]
E	50 V/300 nm[c]
λ_i	12 μeV[d]
ρ	7.5×10^{-7} kg/m^2 [e]
R	35 nm
$U_0 = \Delta$	260 meV
T	100 mK

[a]From Ref. [24].
[b]From Ref. [8].
[c]From Ref. [7].
[d]From Ref. [22].
[e]From Ref. [25].

interaction

$$J_{\gamma_0\gamma_k}(\omega)=\int_{-\infty}^{\infty}dt e^{-i\omega t}\overline{\langle\gamma_0|\mathcal{H}_{\text{s-ph}}(0)|\gamma_k\rangle\langle\gamma_k|\mathcal{H}_{\text{s-ph}}(t)|\gamma_0\rangle}. \tag{29}$$

Further simplifications in Eq. (18) allow us to find the following relation, $1/T_1\propto J_{\gamma_0\gamma_k}(\omega_{\gamma_0\gamma_k})$, where $\omega_{\gamma_0\gamma_k}\propto\omega_Z\propto g\mu_B B$. In a general form, we have that $1/T_1\propto\sum_q K_q\langle\gamma_0|e^{i\mathbf{q}\cdot\mathbf{r}}|\gamma_k\rangle\langle\gamma_k|\mathcal{H}_{\text{SO}}|\gamma_0\rangle\delta(\omega_q-\omega_{\gamma_0\gamma_k})$, where $K_q=q/\sqrt{\omega_q}$ since $\mathcal{H}_{\text{e-ph}}\propto K_q e^{\pm i\mathbf{q}\cdot\mathbf{r}}$. Also, $\sum_q\propto\int dq\,q^{d-1}$, where $d=2$ is the dimensionality of graphene. Each SO coupling defines the selection rule for the quantum number j and, consequently, the order of the dipole expansion as explained in Sec. III. We find that for the Rashba SO coupling, $J_{\gamma_0\gamma_k}(\omega_{\gamma_0\gamma_k})\propto\omega_Z^s$, with $s=4$ for the deformation potential (LA) and $s=2$ for the bond-length change mechanism (LA, TA). Also, for the intrinsic SO, $s\geqslant 2$ for the direct spin-phonon coupling (ZA). Therefore the spectral density of the system-bath interaction is super-Ohmic ($s>1$) with a strong dependence on the bath frequency for all phonons considered in graphene.

V. SPIN DEPHASING RATES

Next we evaluate the spin dephasing rates for all the electron-phonon mechanisms introduced in Sec. III. Within the Bloch-Redfield theory, we can also solve the Bloch equations for the spin components perpendicular to the magnetic field, which are given by $\langle S_x\rangle(t)=S_x^0\cos(\omega_Z t)e^{-t/T_2}$ and $\langle S_y\rangle(t)=S_y^0\sin(\omega_Z t)e^{-t/T_2}$, where $S_{x,y}^0$ are the initial spin polarizations along the x,y directions. The decoherence time can be separated into two contributions: the spin relaxation and the pure spin dephasing $1/T_2=1/2T_1+1/T_\phi$, where the pure spin dephasing rate is [32]

$$\Gamma_\phi=\frac{1}{T_\phi}=\text{Re}\big(\Gamma^+_{\gamma_0\gamma_0\gamma_0\gamma_0}+\Gamma^+_{\gamma_k\gamma_k\gamma_k\gamma_k}-2\Gamma^+_{\gamma_0\gamma_0\gamma_k\gamma_k}\big). \tag{30}$$

In the low-temperature limit, we find that

$$\frac{1}{T_\phi}=\lim_{\omega\to 0}\sum_q|\langle\gamma_0|\mathcal{H}_{\text{s-ph}}|\gamma_0\rangle - \langle\gamma_k|\mathcal{H}_{\text{s-ph}}|\gamma_k\rangle|^2\delta(\hbar\omega-\hbar\omega_q)\frac{2\pi k_b T}{\hbar\omega}. \tag{31}$$

The dephasing time can also be rewritten in terms of the spectral density of the system-bath interaction as $1/T_\phi\propto\lim_{\omega\to 0}J(\omega)\coth(\hbar\omega/2k_bT)\propto\lim_{\omega\to 0}J(\omega)/\omega$.

As we have shown in Sec. III, the spectral function for all electron-phonon coupling mechanisms considered in this work are super-Ohmic. Thus the spin dephasing vanishes in all cases, since $1/T_\phi\propto\lim_{\omega\to 0}\omega^s/\omega\to 0$, with $s>1$. In other words, there are no phonons available in leading order to cause dephasing in graphene quantum dots. The decoherence time T_2 is determined only by the relaxation contribution, i.e., $T_2=2T_1$. Notice that this relation is no longer necessarily true considering two-phonon processes since the combination of emission and absorption energies can fulfill the energy conservation requirement [36]. We predict that the spin decoherence time due to the admixture mechanism will be the dominant mechanism for high magnetic fields $\mathbf{B}>5$ T. That is because the decoherence time in graphene quantum dots due to the hyperfine interaction was predicted to be on the order of tens or hundreds of μs depending on the ^{13}C abundance [5,6] and the orientation of $\mathbf{B}$ [6].

Additionally, the spin dephasing rate could also vanish at the energy anticrossing for a super-Ohmic bath. Within the subspace spanned by the states $\{|1/2,1,\uparrow\rangle,|-1/2,1,\downarrow\rangle\}$, the Hamiltonian $\mathcal{H}$ can be rewritten as $\mathcal{H}_\phi=\Delta_+(B)1+\Delta_-(B)\tau_z$, where τ_z denote a Pauli matrix and $\Delta_\pm=(E_{\gamma_3}\pm E_{\gamma_2})/2$. This magnetic field can be divided into two contributions $B=B_0+\delta B(t)$: an external source B_0 and an internal contribution $\delta B(t)$ due to the bath. For small fluctuations of $\delta B(t)$, the $\mathcal{H}_\phi$ is approximately given by

$$\mathcal{H}_\phi=[\Delta_-(B_0)+\partial_B\Delta_-(B_0)\delta B(t)]\tau_z, \tag{32}$$

where we have not included the term proportional to $\Delta_+\mathbb{1}_{2x2}$ since it does not cause spin dephasing. Calculating the spin dephasing rate within the Bloch-Redfield theory using Eq. (30), we find that

$$\frac{1}{T_\phi}=\left(\frac{2}{\hbar}\partial_B\Delta_-(B_0)\right)^2\lim_{\omega\to 0}\text{Re}\int_0^\infty dt' e^{-i\omega t'}\overline{\langle\delta B(0)\delta B(t')\rangle}, \tag{33}$$

where $\langle A(t)\rangle$ is the thermal equilibrium expectation value of the operator $A(t)$ on the bath. Therefore the spin dephasing rate goes to zero at the energy anticrossing, since $\partial_B\Delta_-(B_0)\to 0$. This condition is valid under the assumption that the thermal average of the fluctuating magnetic field does not diverge. Following the result given by Eq. (31), the spin dephasing rate still vanishes as long as the spectral density of the system-bath interaction is super-Ohmic, i.e., $J(\omega)\propto\omega^s$, with $s>1$.

VI. CONCLUSION

In summary, we find a minimum in the spin relaxation time as a function of the magnetic field that is induced by the Rashba SO coupling and is controllable by an external electric field. In larger quantum dots, the intrinsic SO dominates the spin relaxation over the Rashba SO contribution at low magnetic fields. As the magnetic field increases, the extrinsic contribution takes over, generating a nonmonotonic behavior of T_1 due to the Rashba SO interaction-induced level anticrossing. We have also analyzed the spectral density of the system-bath interaction for the first-order electron-phonon interaction and we have identified a vanishing contribution to the energy-conserving dephasing process. Therefore the phonon-induced pure spin dephasing rate is of the same order of magnitude as the spin relaxation rate, i.e., $T_2=2T_1$, in the leading order of the electron-phonon interaction. Other mechanisms such as nuclear spins from the ^{13}C atoms and charge noise combined with the SO interaction could lead to a nonvanishing spin dephasing rate. We find that the admixture mechanism-induced spin decoherence dominates over the contribution due to the hyperfine interaction [5,6] for high magnetic fields $\mathbf{B}>5$ T. Moreover, we have shown that any super-Ohmic bath has a vanishing spin dephasing rate at the energy anticrossing.

ACKNOWLEDGMENTS

We wish to acknowledge useful discussions with P. R. Struck and Peter Stano. Funding for this work was provided by CNPq, FAPESP, and PRP/USP within the Research Support Center initiative (NAP Q-NANO) (M.O.H. and J.C.E.), and DFG and ESF under Grants No. FOR912 and No. SPP1285, and EuroGraphene (CONGRAN) (G.B.).

APPENDIX: SPIN RELAXATION RATE $\Gamma_{\gamma_1\leftarrow\gamma_2}$

In this Appendix, we demonstrate that the spin relaxation $\Gamma_{\gamma_1\leftarrow\gamma_2}$ is a higher-order contribution in the spin-orbit interaction. Therefore we can neglect $\Gamma_{\gamma_1\leftarrow\gamma_2}$ compared to $\Gamma_{\gamma_0\leftarrow\gamma_2}$ since $\Gamma_{\gamma_1\leftarrow\gamma_2} \ll \Gamma_{\gamma_0\leftarrow\gamma_2}$.

Since we are interested in the transition from the excited state γ_2 to γ_1, we calculate the matrix element of the effective spin-phonon Hamiltonian $\langle\gamma_1|\mathcal{H}^R_{\text{s-ph}}|\gamma_2\rangle = \langle\gamma_1|\mathcal{H}_{\text{e-ph}} + [\mathcal{S}^R,\mathcal{H}_{\text{e-ph}}]|\gamma_2\rangle$ using Eq. (9). In terms of the matrix elements of the spin-orbit coupling and electron-phonon interaction, we find

$$\begin{aligned}\langle\gamma_1|\mathcal{H}^R_{\text{s-ph}}|\gamma_2\rangle &= \cos(\vartheta/2)\sin(\vartheta/2)\Lambda_0(\mathcal{H}_{\text{e-ph}},\mathcal{H}_{\text{e-ph}}) + \sum_{n',s\neq\mathfrak{D}}\frac{1}{E_{\gamma_2}-E_{n'}}[\cos(\vartheta/2)^2 e^{-i\delta}\Lambda_1(\mathcal{H}_{\text{e-ph}},\mathcal{H}_R)\\ &\quad - \sin(\vartheta/2)^2 e^{+i\delta}\Lambda_2(\mathcal{H}_{\text{e-ph}},\mathcal{H}_{\text{R}})] + \sum_{n',s\neq\mathfrak{D}}\frac{1}{E_{\gamma_2}-E_{n'}}[\cos(\vartheta/2)^2 e^{-i\delta}\Lambda_1(\mathcal{H}_R,\mathcal{H}_{\text{e-ph}})\\ &\quad - \sin(\vartheta/2)^2 e^{+i\delta}\Lambda_2(\mathcal{H}_R,\mathcal{H}_{\text{e-ph}})] + O\left(\mathcal{H}^2_{\text{SO}}\right),\end{aligned} \tag{A1}$$

where the degenerate subspace is given by $\mathfrak{D} = \{|1/2,1,\uparrow\rangle,|-1/2,1,\downarrow\rangle\}$. Here, we define

$$\Lambda_0(\mathcal{H}_i,\mathcal{H}_j) = \langle 1/2,1,\uparrow|\mathcal{H}_i|1/2,1,\uparrow\rangle - \langle -1/2,1,\downarrow|\mathcal{H}_j|-1/2,1,\downarrow\rangle, \tag{A2}$$

$$\Lambda_1(\mathcal{H}_i,\mathcal{H}_j) = \langle 1/2,1,\uparrow|\mathcal{H}_i|n',s\rangle\langle n',s|\mathcal{H}_j|-1/2,1,\downarrow\rangle, \tag{A3}$$

$$\Lambda_2(\mathcal{H}_i,\mathcal{H}_j) = \langle -1/2,1,\downarrow|\mathcal{H}_i|n',s\rangle\langle n',s|\mathcal{H}_j|1/2,1,\uparrow\rangle. \tag{A4}$$

Also, $i,j = \text{e-ph},R$ denotes the index for the electron-phonon and spin-orbit Hamiltonians, respectively. The terms $\mathcal{H}_{\text{e-ph}}$ and $\mathcal{H}_R$ only connect states with an angular quantum number such that $|j-j'| = 1$ [26]. Thus $\Lambda_0(\mathcal{H}_{\text{e-ph}},\mathcal{H}_{\text{e-ph}})$ vanishes since this term does not fulfill the selection rules for j. Note in addition that only terms $\Lambda_{1,2}(\mathcal{H}_i,\mathcal{H}_j)$ such as $\langle j,\nu,s|\mathcal{H}_{\text{e-ph}}|j\pm1,\nu',s\rangle\langle j\pm1,\nu',s|\mathcal{H}_R|(j\pm1)\pm1,\nu'',s'\rangle$ with $s\neq s'$ are nonzero. However, there are no such terms in Eq. (A1). Thus $\langle\gamma_1|\mathcal{H}^R_{\text{s-ph}}|\gamma_2\rangle$ vanishes in the first order in the spin-orbit interaction, i.e., $\langle\gamma_1|\mathcal{H}^R_{\text{s-ph}}|\gamma_2\rangle \propto O(\mathcal{H}^2_{\text{SO}})$ and $\Gamma_{\gamma_1\leftarrow\gamma_2} \propto O(\mathcal{H}^4_{\text{SO}})$. As a consequence, $\Gamma_{\gamma_1\leftarrow\gamma_2} \ll \Gamma_{\gamma_0\leftarrow\gamma_2}$, as stated in Sec. IV. Notice that these types of matrix elements in Eq. (A1) vanish for all types of electron-phonon interactions.

[1] A. H. Castro Neto, F. Guinea, N. M. R. Peres, K. S. Novoselov, and A. K. Geim, Rev. Mod. Phys. **81**, 109 (2009).

[2] D. Loss and D. P. DiVincenzo, Phys. Rev. A **57**, 120 (1998).

[3] B. Trauzettel, D. V. Bulaev, D. Loss, and G. Burkard, Nat. Phys. **3**, 192 (2007).

[4] D. P. DiVincenzo, Fortschr. Phys. **48**, 771 (2000).

[5] J. Fischer and B. Trauzettel, and D. Loss. Phys. Rev. B **80**, 155401 (2009).

[6] M. Fuchs, V. Rychkov, and B. Trauzettel, Phys. Rev. B **86**, 085301 (2012).

[7] C. L. Kane and E. J. Mele, Phys. Rev. Lett. **95**, 226801 (2005).

[8] H. Min, J. E. Hill, N. A. Sinitsyn, B. R. Sahu, L. Kleinman, and A. H. MacDonald, Phys. Rev. B **74**, 165310 (2006).

[9] H. O. H. Churchill, F. Kuemmeth, J. W. Harlow, A. J. Bestwick, E. I. Rashba, K. Flensberg, C. H. Stwertka, T. Taychatanapat, S. K. Watson, and C. M. Marcus, Phys. Rev. Lett. **102**, 166802 (2009).

[10] D. V. Bulaev, B. Trauzettel, and D. Loss, Phys. Rev. B **77**, 235301 (2008).

[11] M. S. Rudner and E. I. Rashba, Phys. Rev. B **81**, 125426 (2010).

[12] D. V. Bulaev and D. Loss, Phys. Rev. B **71**, 205324 (2005).

[13] P. Stano and J. Fabian, Phys. Rev. B **72**, 155410 (2005).

[14] P. Stano and J. Fabian, Phys. Rev. B **74**, 045320 (2006).

[15] S. Y. Zhou, G.-H. Gweon, A. V. Fedorov, P. N. First, W. A. de Heer, D.-H. Lee, F. Guinea, A. H. Castro Neto, and A. Lanzara, Nat. Mater. **6**, 770 (2007).

[16] G. Giovannetti, P. A. Khomyakov, G. Brocks, P. J. Kelly, and J. van den Brink, Phys. Rev. B **76**, 073103 (2007).

[17] J. Slawinska, I. Zasada, P. Kosinski, and Z. Klusek, Phys. Rev. B **82**, 085431 (2010).

[18] P. Recher, J. Nilsson, G. Burkard, and B. Trauzettel, Phys. Rev. B **79**, 085407 (2009).

[19] The single-valley approximations hold since the valley splitting $\Delta E_{K,K'}$ for the ground state is much larger than the intervalley coupling $\Delta_{K,K'}$ even for a very small magnetic field. For instance, we find that $\Delta E_{K,K'} \sim 10^2$ meV $\gg \Delta_{K,K'} \sim 10$ meV [9, 20] for $\mathbf{B} = 0.05$ T. Thus our results are valid for $\mathbf{B} > \mathbf{B}_{\text{crit}}$, where we estimate the critical external magnetic field as $\mathbf{B}_{\text{crit}} = 0.05$ T.

[20] A. Palyi, P. R. Struck, M. Rudner, K. Flensberg, and G. Burkard, Phys. Rev. Lett. **108**, 206811 (2012).
[21] The tensor product notation is implicit, i.e., $\sigma_i s_j \equiv \sigma_i \otimes s_j$, for $i,j = x,y,z$.
[22] M. Gmitra, S. Konschuh, C. Ertler, C. Ambrosch-Draxl, and J. Fabian, Phys. Rev. B **80**, 235431 (2009).
[23] D. Huertas-Hernando, F. Guinea, and A. Brataas, Phys. Rev. B **74**, 155426 (2006).
[24] T. Ando, J. Phys. Soc. Jpn. **74**, 777 (2005).
[25] L. A. Falkovsky, Phys. Lett. A **372**, 5189 (2008); J. Exp. Theor. Phys. **105**, 397 (2007).
[26] P. R. Struck and G. Burkard, Phys. Rev. B **82**, 125401 (2010).
[27] R. Winkler, *Spin-Orbit Coupling Effects in Two-Dimensional Electron and Hole Systems* (Springer, Berlin, 2003).
[28] V. N. Golovach, A. Khaetskii, and D. Loss, Phys. Rev. Lett. **93**, 016601 (2004).
[29] We do not carry the term $[\mathcal{S},\mathcal{H}_{\rm ph}]$ since it does not contribute to the effective spin-phonon Hamiltonian, i.e., $\langle\gamma_0|\mathcal{H}_{\rm ph} + [\mathcal{S},\mathcal{H}_{\rm ph}]|\gamma_k\rangle = 0$.
[30] The matrix elements of the Rashba SO and all the electron-phonon coupling mechanisms are presented in Ref. [26].
[31] K. Blum, *Density Matrix Theory and Applications*, 2nd ed. (Springer, New York, 2012).
[32] L. Chirolli and G. Burkard, Adv. Phys. **57**, 225 (2008).
[33] J. H. van Vleck, Phys. Rev. **57**, 426 (1940).
[34] In GaAs quantum dots, the spin relaxation occurs within a Kramers pair $|n\downarrow\rangle$ and $|n\uparrow\rangle$ where these two states are related by time reversal. As a consequence, the matrix element of the effective spin-phonon Hamiltonian $\langle n\downarrow|\mathcal{H}_{\text{s-ph}}|n\downarrow\rangle = \langle n\uparrow|[\mathcal{S},\mathcal{H}_{\text{e-ph}}]|n\downarrow\rangle$ vanishes at $B = 0$. At zero magnetic field, the term $\langle m\downarrow|\mathcal{H}_{\text{s-ph}}|m\downarrow\rangle$ can be rewritten as two terms, as shown in Eq. (4) of Ref. [26], which cancel out (Van Vleck cancellation). This statement can be proven using the symmetry of the matrix elements of the SO coupling and the electron-phonon interaction under the exchange of indexes n and n', i.e., $\langle m\downarrow|\mathcal{H}_{\rm SO}|m'\uparrow\rangle = -\langle m'\downarrow|\mathcal{H}_{\rm SO}|m\uparrow\rangle$ and $\langle ms|\mathcal{H}_{\text{e-ph}}|m's\rangle = \langle m's|\mathcal{H}_{\text{e-ph}}|ms\rangle$. It leads to a vanishing spin relaxation rate at $B = 0$, as found in Ref. [35]. In contrast, we are restricting ourselves to a single valley K in a graphene quantum dot since the valley degeneracy is broken by the mass term Δ and a very small magnetic field **B** (see Refs. [18, 19]). Thus our spin qubit does not form a Kramers pair. Hence, the Van Vleck cancellation does not apply and we expect a finite value for T_1 for very small magnetic fields as long as the single-valley approximation still holds [19].
[35] A. V. Khaetskii and Yu. V. Nazarov, Phys. Rev. B **64**, 125316 (2001).
[36] M. Trif, P. Simon, and D. Loss, Phys. Rev. Lett. **103**, 106601 (2009).